

Non-orthogonal multiple access with phase pre-distortion in visible light communication

XUN GUAN,¹ QING YANG,^{2,*} YANG HONG,¹ AND CALVIN CHUN-KIT CHAN¹

¹Department of Information Engineering, The Chinese University of Hong Kong, Shatin, N.T., Hong Kong, China

²P2 Wireless Technologies, Units 501-502, Building 12W, Hong Kong Science Park, N.T., Hong Kong, China

*yang.qing@hotmail.com

Abstract: Non-orthogonal multiple access (NOMA) offers a good balance between throughput and fairness for visible light communication (VLC). This work presents a phase pre-distortion method to improve the symbol error rate performance of NOMA uplink with successive interference cancellation (SIC) decoding in VLC. Both theoretical analysis and experimental evaluation have shown that the proposed phase pre-distortion method improves the bit-error-rate (BER) performance for NOMA under both low and high relative power ratios. Specifically, at low relative power ratios, the proposed method can eliminate the possible BER floors and alleviate the power ratio requirement by 2 dB at the BER of 3.8×10^{-3} .

© 2016 Optical Society of America

OCIS codes: (060.0060) Fiber optics and optical communications; (060.2605) Free-space optical communication; (230.3670) Light-emitting diodes; (060.4230) Multiplexing.

References and links

1. A. Jovicic, J. Li, and T. Richardson, "Visible light communication: opportunities, challenges and the path to market," *IEEE Commun. Mag.* **51**(12), 26–32 (2013).
2. M. Biagi, A. M. Vegni, and T. D. C. Little, "LAT indoor MIMO-VLC localize, access and transmit," in *IEEE International Workshop on Wireless Optical Communications* (IEEE, 2012).
3. Y. Saito, Y. Kishiyama, A. Benjebbour, T. Nakamura, A. Li, and K. Higuchi, "Non-orthogonal multiple access (NOMA) for cellular future radio access," in *Proceedings of IEEE Vehicular Technology Conference* (IEEE, 2013), pp. 1–5.
4. L. Dai, B. Wang, Y. Yuan, S. Han, C. i, and Z. Wang, "Non-orthogonal multiple access for 5G: solutions, challenges, opportunities, and future research trends," *IEEE Commun. Mag.* **53**(9), 74–81 (2015).
5. Y. Endo, Y. Kishiyama, and K. Higuchi, "Uplink non-orthogonal access with MMSE-SIC in the presence of inter-cell interference," in *Proceedings of International Symposium on Wireless Communication Systems* (IEEE 2012), pp. 261–265.
6. J. Schaefferle and A. Ruegg, "Enhancement of throughput and fairness in 4G wireless access systems by non-orthogonal signaling," *Bell Labs Tech. J.* **13**(4), 59–77 (2009).
7. H. Marshoud, V. M. Kapinas, G. K. Karagiannidis, and S. Muhaidat, "Non-orthogonal multiple access for visible light communications," *IEEE Photonics Technol. Lett.* **28**(1), 51–54 (2016).
8. R. C. Kizilirmak, C. R. Rowell, and M. Uysal, "Non-orthogonal multiple access (NOMA) for indoor visible light communications," in *Proceedings of International Workshop on Optical Wireless Communications* (IWOW 2015), pp. 98–101.
9. H. Haas, L. Yin, Y. Wang, and C. Chen, "What is LiFi?" *J. Lightwave Technol.* **34**(6), 1533–1544 (2016).
10. X. Guan, Y. Hong, Q. Yang, and C. C. K. Chan, "Phase pre-distortion for non-orthogonal multiple access in visible light communications," in *Optical Fiber Communication Conference* (OFC, 2016), paper Th1H.4.
11. S. D. Dissanayake and J. Armstrong, "Comparison of ACO-OFDM, DCO-OFDM and ADO-OFDM in IM/DD systems," *J. Lightwave Technol.* **31**(7), 1063–1072 (2013).

1. Introduction

Visible light communication (VLC) is an emerging technique of optical wireless communication. With its advantages of license-free, low cost, and easy integration with pervasive illumination devices, VLC has been considered as a feasible candidate for 5G cellular system as well as a potential complement of radio frequency (RF) communications [1], especially for indoor access [2]. To support optical wireless networks with multiple VLC transmitters and receivers, a designated multiple access method is indispensable. Recently, a new multiple access technology, named non-orthogonal multiple access (NOMA), has

attracted much research attention, as it offers a better balance between system fairness and throughput [3, 4]. Unlike the conventional multiple access methods, NOMA allows multiple wireless users to simultaneously transmit their signals, via the same frequency band, to a common receiver, resulting in signal overlapping in both time and frequency domains, as well as signal multiplexing in the power domain.

In wireless multiple access systems, randomly distributed users are connected to the access points (AP) with different channel gains, owing to different transmission distances. Near users enjoy high signal-to-noise ratio (SNR) and better performance, while far users suffer from low SNR and poor performance. By applying NOMA to orthogonal frequency division multiple access (OFDMA) systems, a better balance between system fairness and throughput [5] is realized. When the near and the far users are granted concurrent uplink access to the same subcarrier, fairness is assured by keeping the far users served, while maintaining the throughput of the near users by allocating more subcarriers to them. Moreover, NOMA improves the system capacity. Previous works reported that the sum throughput of time division multiple access (TDMA) uplinks and downlinks could be significantly improved by applying NOMA, and a higher channel gain difference yielded a larger improvement [6].

Apart from the applications in wireless communications, NOMA is also a very promising multiple access method for VLC, with good feasibility and performance, thus has attracted much research attention [7–9]. In this paper, we extend our work in [10], in which a novel phase pre-distortion scheme was proposed to improve the system performance of NOMA in VLC. Here, we further comprehensively characterize the phase pre-distorted NOMA system in VLC both theoretically and experimentally.

The rest of this paper is organized as follows. Section II describes the system model, while Section III illustrates the principles of the proposed phase pre-distorted NOMA scheme. Section IV presents the experimental evaluations and Section V summarizes the paper.

2. System model

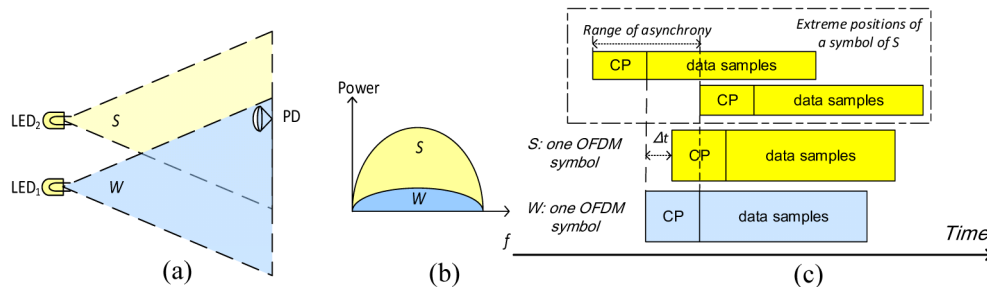


Fig. 1. (a) System model for the non-orthogonal multiple access in visible light communication; (b) power levels of S and W ; (c) time asynchrony in NOMA.

Figure 1(a) depicts a typical VLC system supporting NOMA in the uplink of a multiple access system. Two light emitting diodes (LED), namely LED₁ and LED₂, are the uplink transmitters while a photodiode (PD) acts as the multiple access receiver. The two LEDs and the PD are located at fixed positions. The PD lies at the center of the illuminated region of LED₂, but at the edge of the illuminated region of LED₁, thus it receives a stronger signal S from LED₂ but a weaker signal W from LED₁, simultaneously, forming a composite signal C . Figure 1(b) shows the power levels of S and W . Both S and W employ OFDM format, in which the transmission band is divided into N subcarriers. The n^{th} time-domain sample in one OFDM symbol is

$$x(n) = \sum_{k=0}^{N-1} \left(X(k) \cdot e^{j2\pi \frac{kn}{N}} \right), \text{ for } n \in (0, N-1], n \in Z, \quad (1)$$

where $X(k)$ is the symbol on the k^{th} subcarrier, and $X^*(k)$ denotes its complex conjugate. Since the OFDM signal is intensity-modulating the LED, the two sidebands of a real-valued signal are Hermitian symmetric in frequency-domain, i.e., $X(k) = X^*(N-k)$. The bipolar signal $x(n)$ could be modulated onto the amplitude of an LED by discrete current optical OFDM (DCO-OFDM) [11].

In practice, S and W may arrive at PD with a random time asynchrony, which is due to the practical implementation of the VLC system, such as different transmission times, different hardware processing times, different transmission distances, and multipath effect. This asynchrony could be tolerated by appending cyclic prefix (CP) to each OFDM symbol, which is a common practice in OFDMA. As illustrated in Fig. 1(c), time asynchrony within the CP length can be accommodated.

Assume the misalignment between S and W is m samples (m is not necessarily an integer), the signal C has been synchronized and CP is cut down with respect to the frame duration of signal S . Denote the signals S and W , as well as the composite signal C by subscripts s , w , and c , respectively. Ignore the noise term, the n^{th} sample in one symbol of the signal C received at PD is given by

$$x_c(n) = x_s(n) * h_s(n) + x_w(n+m) * h_w(n), \quad (2)$$

where the symbol $*$ stands for convolution; $h_s(\cdot)$ and $h_w(\cdot)$ are the time-domain channel impulse responses between LED₁ and PD, as well as that between LED₂ and PD, respectively. After *fast Fourier transform* (FFT), denoted by F , on both sides, Eq. (2) becomes

$$X_c(k) = F\{x_c(n)\} = X_s(k)H_s(k) + X_w(k)H_w(k)e^{j2\pi\frac{km}{N}}, \quad (3)$$

where $H_s(k)$ and $H_w(k)$ are the respective frequency domain channel responses on the k^{th} subcarrier of S and W , which are estimated separately using training sequences that do not overlap in the time domain.

Upon receiving the overlapped signal C in time domain as x_c and recovering X_c by FFT, successive interference cancellation (SIC) is employed to detect the individual signals sent from LED₁ and LED₂. The SIC process consists of two steps: (1) the strong signal X_s is decoded while treating the weak signal component, X_wH_w , as noise; (2) the term X_sH_s is reconstructed and subtracted from Y_c before the weak signal X_w is decoded.

3. Phase pre-distortion for successive interference cancellation in NOMA

Assume that each of the signals S and W is quadrature phase state keying (QPSK) modulated with four constellation points $(\sqrt{2}/2)\{1+i, -1+i, -1-i, 1-i\}$. Without loss of generality, we consider one subcarrier at the receiver. Ignore the index k and absorb the exponential term into H_w , Eq. (3) can be reformulated as

$$Y_c = X_sH_s + X_wH_w. \quad (4)$$

To ease the presentation, we define

$$\frac{H_s}{H_w} = re^{j\varphi}, r_{dB} = 20\lg(r), \quad (5)$$

where r denotes the amplitude ratio of the two channel coefficients, and r_{dB} is the power ratio expressed in dB scale; φ denotes the relative phase difference between the channel coefficients H_w and H_s . We model φ by a uniformly distributed random variable over $\varphi \in (0, 2\pi]$. Let P_{e1} and P_{e2} denote the symbol error rate (SER) in step (1) and step (2) of SIC, respectively. Also, let P_m denotes the probability that the strong user (S) transmits a symbol $m \in (\sqrt{2}/2)\{1+i, -1+i, -1-i, 1-i\}$, and P_n denotes the probability that the weak user

(W) transmits a symbol $n \in (\sqrt{2}/2)\{1+i, -1+i, -1-i, 1-i\}$. Assume all the messages are equi-probable, i.e., $P_m = P_n = 1/4$. In addition, let P_{mn} denotes the probability that S contains message m while W contains n . The SER in SIC step (1) is

$$P_{e1} = \sum_{m=1}^4 P_m \sum_{n=1}^4 P_n P_{e|mn}, \quad (6)$$

where $P_{e|mn}$ denotes the error probability of S containing message m and W containing message n , while $P_{c|mn}$ as the respective correct decision of m and n . As the in-phase noise and the quadrature-phase noise are orthogonal and independent, the error probability $P_{e|mn}$ can be expressed as

$$P_{e|mn} = 1 - P_{c|mn} = 1 - P_{Ic|mn} P_{Qc|mn} = P_{Ie|mn} + P_{Qe|mn} - P_{Ie|mn} P_{Qe|mn}, \quad (7)$$

where $P_{Ie|mn}$ and $P_{Qe|mn}$ are the error probabilities of the in-phase dimension and quadrature-phase dimension, respectively. These two terms can be given by

$$P_{Ie|mn} = Q\left(\frac{\text{Re}\{s_{mn}\}}{\sqrt{N_0}/2}\right) \quad P_{Qe|mn} = Q\left(\frac{\text{Im}\{s_{mn}\}}{\sqrt{N_0}/2}\right), \quad (8)$$

where $Q(\cdot)$ denotes the Q -function; N_0 denotes the noise spectral density, supposing an additive white Gaussian noise (AWGN) channel. Therefore,

$$\begin{aligned} P_{e1} &= \sum_{m=1}^4 P_m \sum_{n=1}^4 P_n P_{e|mn} = \sum_{m=1}^4 P_m \sum_{n=1}^4 P_n (P_{Ie|mn} + P_{Qe|mn} - P_{Ie|mn} \cdot P_{Qe|mn}) \\ &= \frac{1}{4} \sum_{n=1}^4 \left\{ Q\left(\frac{\frac{\sqrt{2}}{2} + r \cos(\varphi + \frac{n\pi}{2} - \frac{\pi}{4})}{\sqrt{N_0}/2}\right) + Q\left(\frac{\frac{\sqrt{2}}{2} + r \sin(\varphi + \frac{n\pi}{2} - \frac{\pi}{4})}{\sqrt{N_0}/2}\right) \right. \\ &\quad \left. - Q\left(\frac{\frac{\sqrt{2}}{2} + r \cos(\varphi + \frac{n\pi}{2} - \frac{\pi}{4})}{\sqrt{N_0}/2}\right) \cdot Q\left(\frac{\frac{\sqrt{2}}{2} + r \sin(\varphi + \frac{n\pi}{2} - \frac{\pi}{4})}{\sqrt{N_0}/2}\right) \right\}. \end{aligned} \quad (9)$$

Meanwhile, the error probability of SIC in step (2) is

$$\begin{aligned} P_{e2} &= P_{e1} + (1 - P_{e1}) \left[2Q\left(\frac{1}{r\sqrt{N_0}}\right) - Q^2\left(\frac{1}{r\sqrt{N_0}}\right) \right] \\ &= \left\{ 1 - \left[2Q\left(\frac{1}{r\sqrt{N_0}}\right) - Q^2\left(\frac{1}{r\sqrt{N_0}}\right) \right] \right\} P_{e1} + 2Q\left(\frac{1}{r\sqrt{N_0}}\right) - Q^2\left(\frac{1}{r\sqrt{N_0}}\right). \end{aligned} \quad (10)$$

Therefore, P_{e2} is monotonically increasing with respect to P_{e1} . In addition, an error in SIC step (1) would inevitably lead to an error in SIC step (2). Thus, it is crucial to reduce the value of P_{e1} .

As the overlapped constellation is centrosymmetric with respect to the origin, we only compute the error probability of the constellation points in the first quadrant. Moreover, as the overlapped constellation is also rotational symmetry, we only consider $\varphi \in (-\pi/4, 0]$. The optimal phase difference φ_{opt} is obtained by

$$\varphi_{opt} = \arg \min_{\varphi} P_{e1}, \quad \varphi \in (-\pi/4, 0]. \quad (11)$$

Assume r is 1.41 ($r_{dB} = 3$ dB). By numerical analysis, the value of P_{e1} with respect to the relative phase difference φ is plotted in Fig. 2(a). Our numerical analysis shows that the optimal phase difference is $\varphi_{opt} = 0$, which is also applicable to other r values. Hence, it can be

seen that P_{e1} does not stay constant with regard to φ . It can be deduced that the BER can be reduced by pre-distorting the transmitted signals to the optimal phase difference $\varphi_{opt} = 0$. Figures 2(b) and 2(c) compare the constellations without and with phase pre-distortion, respectively.

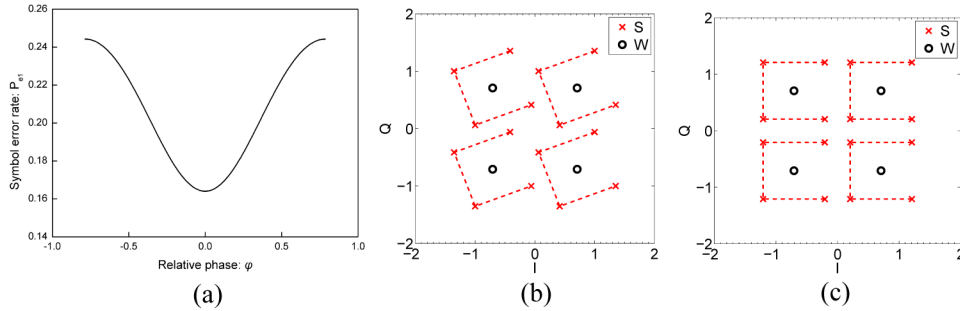


Fig. 2. (a) The symbol error rate (P_{e1}) in step (1) of successive interference cancellation decoding versus the phase difference between the two users that both adopt QPSK modulation when $r = 1.41$ ($r_{dB} = 3$ dB); (b) an example of constellations without phase pre-distortion; (c) constellations with phase pre-distortion corresponding to (b).

4. Experiments

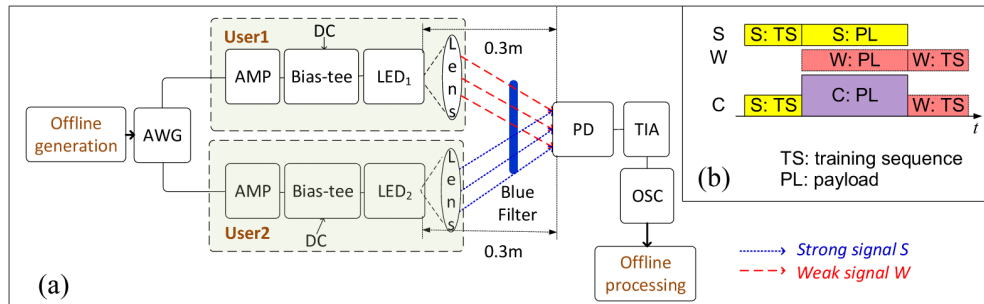


Fig. 3. (a) Experimental Setup to evaluate the proposed phase pre-distortion method, AWG: arbitrary waveform generator, AMP: amplifier, DC: direct current, LED: lighting emitted diode, PD: photodiode, TIA: trans-impedance amplifier, DSO: digital storage oscilloscope; (b) frame format for the NOMA users.

Figure 3(a) shows the experimental setup to evaluate the proposed phase pre-distortion method for NOMA in VLC. In conventional NOMA uplink transmission, the signal transmission was in a single phase without any prior training sequences. The signals were directly transmitted without any channel state information (CSI) feedback. Two transmitted signals were generated, via an arbitrary waveform generator (AWG), and were amplified by the amplifiers (AMP), before being fed to the LEDs (OSRAM LUW W5AM), via two bias tees, respectively. A lens was mounted in front of each LED so as to focus the respective output light to a common photodiode (HAMAMATU S10784) placed behind a blue filter. The distance between each LED and the PD was fixed to be 0.3 meter. During the experiment, the received signal powers from both LEDs, as well as their relative power ratios were adjusted by tuning the respective driving signal amplitudes of the LEDs. On the receiver side, we first amplified the received signal from the PD by a trans-impedance amplifier (TIA), and then fed it to an oscilloscope (DSO) for data acquisition and offline processing. Each OFDM frame comprised 10 training symbols for channel estimation and 240 payload symbols for data transmission. For each OFDM symbol, the FFT size was 256, and the cyclic prefix (CP) length was 32. The two subcarriers next to the DC level were nulled, owing to the DC block of the bias tees. The sampling rates of the AWG and the DSO were 100 MSa/s and 250

MSa/s, respectively. To avoid collision of training symbols, the signal frames of S and W were designed, as illustrated in Fig. 3(b).

We added a random within-CP delay at user 1 to produce a random phase shift between the two signals. While conventional NOMA suffered from the random phase shift, our newly proposed scheme pre-distorted the phase difference to φ_{opt} . In conventional NOMA uplink, the signal transmission was in one-phase process without training transmission, while the proposed phase pre-distorted NOMA case was a two-phase process. In the first phase, each user transmitted a training sequence to the receiver, where the CSI was estimated, based on the training sequence, and fed back to the respective user. In the second phase, each user pre-distorted its payload, based on the CSI acquired in the first phase, before being sent over the VLC system, similar to the conventional NOMA case.

5. Experimental results and discussion

Figures 4(a)-4(c) shows the measured BER as a function of the SNR of the strong signal S , under different relative power ratios between S and W , i.e., r_{dB} . It could be observed that the proposed pre-distorted NOMA scheme substantially reduced the BERs of both signals S and W , compared to the conventional NOMA scheme under all power ratios of both signals S and W . For example in Fig. 4(b), when r_{dB} was 4.2 dB, with pre-distortion, BERs of S and W could drop below the threshold when the SNR of S was greater than 17.2 dB. However, the conventional NOMA still could not meet the required BER for FEC, even when the SNR of S was greater than 20.5 dB.

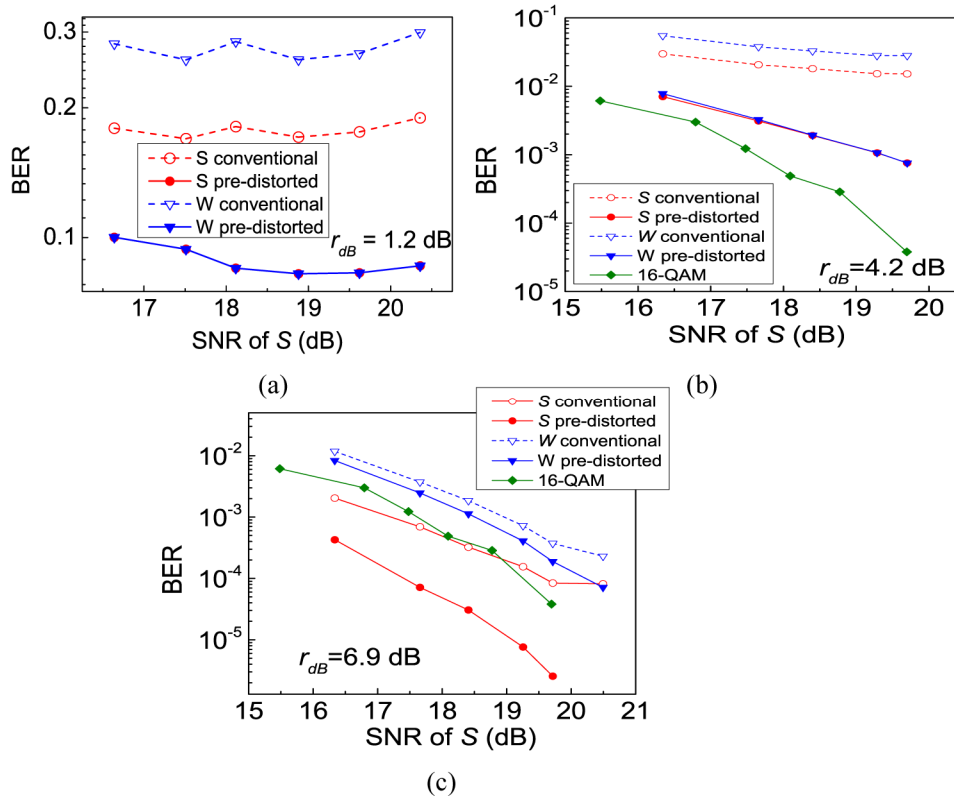


Fig. 4. (a)-(c) Bit error rate (BER) versus the SNR of the strong signal (S). The power ratios r_{dB} between the strong signal and the weak signal are fixed to be (a) 1.2 dB, (b) 4.2 dB, and (c) 6.9 dB.

By keeping the SNR of S to a fixed value and changing the relative power ratio between S and W , the BER of S and W along with the variation of the relative power ratio is depicted in

Fig. 5. When the SNR of S was 20.5 dB, with the adoption of phase pre-distortion, the minimum r_{dB} for individual signal S and W to reach the threshold was reduced by 2.1 and 1.9 dB, respectively, compared to the conventional NOMA. The increase in the BER of signal W at high r_{dB} could be attributed to the insufficient SNR of W . Figures 6(a) and 6(b) show the received signal constellations of the conventional and phase pre-distorted NOMA when S and W both adopted QPSK modulation. It could be seen that in the phase pre-distorted NOMA, the constellation was an irregular 16-QAM which largely avoided the marginal areas of four quadrants, and tended to incur decoding errors in step (1) of SIC.

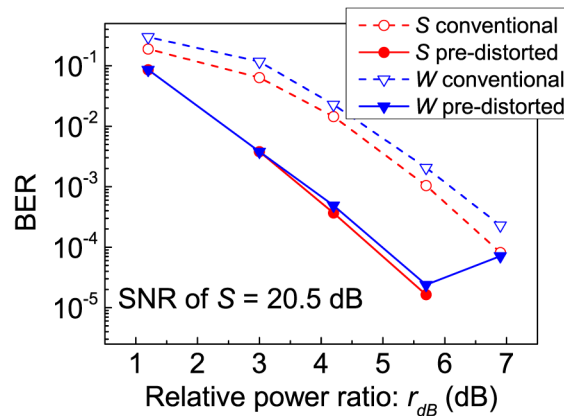


Fig. 5. Bit error rate (BER) versus the power ratio (r_{dB}) between the strong signal (S) and the weak signal (W) when the SNR of S is fixed to be 20.5 dB.

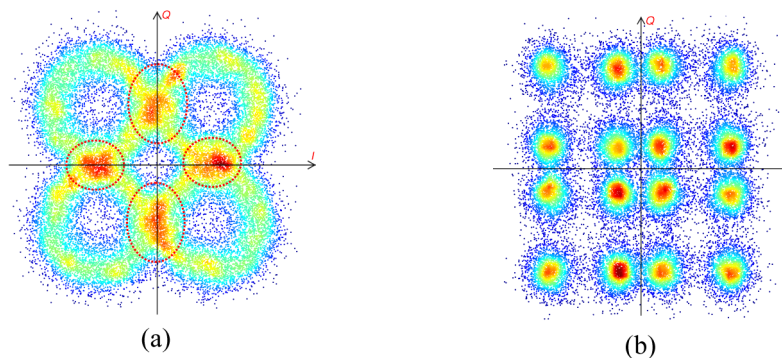


Fig. 6. Examples of the received signal constellations when S and W adopted QPSK modulation at $r_{dB} = 4.2$ dB, with the scheme of (a) conventional NOMA, (b) phase pre-distorted NOMA.

6. Summary

We have proposed a phase pre-distortion method for NOMA uplink with SIC decoding in VLC systems. This method improves the BER performance of SIC decoding by maximizing the minimum distance of the received signal constellation under NOMA. With the retrieved channel state information, the users can compute the optimal phase pre-distortion term, which is then used to pre-distort the phases of the individual signals, accordingly, prior to transmission. Experimental results showed that the proposed phase pre-distortion method improved the BER performance under low, medium, and high relative power ratios between both signals, compared to the conventional NOMA scheme. In particular, the phase pre-distorted NOMA eliminated the BER error floors as in the conventional NOMA uplink case,

at low relative power ratios and also alleviated the relative power ratio requirement by around 2 dB, so as to achieve a BER of 3.8×10^{-3} .

Funding

Hong Kong Research Grants Council GRF Project (No. 14200614); AoE Grant (E- 02/08).